Available online at www.sciencedirect.com

SciVerse ScienceDirect

Ceramics International 39 (2013) 1841–1851

CERAMICS INTERNATIONAL

www.elsevier.com/locate/ceramint

Structure and oxidation resistance of micro-cellular Si–SiC foams derived from natural resins

G. Amaral-Labat[a,b], C. Zollfrank[c,d], A. Ortona[e], S. Pusterla[e], A. Pizzi[a,f], V. Fierro[b], A. Celzard[a,b,*]

[a]*Université de Lorraine. ENSTIB, 27 rue Philippe Séguin, BP 1041, 88051 Épinal cedex 9, France*
[b]*Institut Jean Lamour—UMR CNRS 7198. ENSTIB, 27 rue Philippe Séguin, BP 1041, 88051 Épinal cedex 9, France*
[c]*Biogene Polymere, Technische Universität München, WZ Straubing, Schulgasse 16, D-94315 Straubing, Germany*
[d]*Department of Materials Science and Engineering, University Erlangen-Nuremberg, Martensstr. 5, 91058 Erlangen, Germany*
[e]*University of Applied Sciences (SUPSI): The iCIMSI Research Institute, Department of Technology and Innovation, Galleria 2, 6928 Manno, Switzerland*
[f]*LERMAB—EA 4370. ENSTIB, 27 rue Philippe Séguin, BP1041, 88051 Epinal cedex 9, France*

Received 6 July 2012; received in revised form 9 August 2012; accepted 10 August 2012
Available online 17 August 2012

Abstract

Microcellular Si–SiC porous ceramics were prepared from rigid foams derived from tannin-based natural resins. Such natural foams were used either as such, i.e. in the "green" state, or after conversion at 900 °C into vitreous cellular carbon foams. Various preparation methods were tested: replica with preceramic polymers followed by pyrolysis, liquid silicon infiltration (LSI) and vapour silicon infiltration (VSI). Depending on the method, very different materials have been obtained, whose morphology and microstructure have been investigated by SEM, XRD and Raman, whereas oxidation resistance has been evaluated by weight loss measurements in dry air at high temperature. The resulting porous ceramics' properties were discussed in relation to the preparation methods and their morphology and conversion of tannin-based foams into SiC.

Keywords: Precursors: Microstructure-final; Thermal conductivity; SiC

1. Introduction

Open cellular ceramics are highly porous materials characterised by an array of interconnected empty cells with solid edges. The structure of a cellular ceramic can be described as a stack of polyhedra arranged to efficiently fill the space. In the case of ceramic foams, cells are random in size and orientation [1]. Many works in the literature have demonstrated that cellular ceramics properties are independent from their cell size. It is also true that, for a given cell size, the thickness of the struts affects the resulting material's relative density and thus its properties. It is then easy to conclude that highly porous microcellular ceramic foams must have extremely thin struts. There are only a few manufacturing techniques which are able to produce such kind of materials with exploitable properties, and even less if the ceramic material must be silicon carbide [2].

Silicon carbide is a very important compound of the ceramic industry, given the numerous qualities that combine outstanding thermal stability, high thermal conductivity, superior mechanical resistance at high temperature, low coefficient of thermal expansion, and excellent resistance to thermal shocks and to abrasion. Macroporous silicon carbide foams have been used in applications working at high temperatures ($>$ 1000 °C) and harsh environments because of their unique properties [3,4]. These applications can be divided in two categories. One takes advantage of the peculiar cellular morphology of their bulk material [5] and concerns thermo-mechanical [6] and electrical [7] applications. The other one exploits the properties of their high interconnected porosity: porous burners [8–11], catalyst

*Corresponding author at: Université de Lorraine, BP 1041, 27 rue Philippe Séguin, Épinal cedex 9, 88051 Épinal cedex, France.
Tel.: +33 329 29 61 14; fax: +33 329 29 61 38.
E-mail address: Alain.Celzard@enstib.uhp-nancy.fr (A. Celzard).

0272-8842/$ - see front matter © 2012 Elsevier Ltd and Techna Group S.r.l. All rights reserved.
http://dx.doi.org/10.1016/j.ceramint.2012.08.032

supports [12,13], molten metal filters [7], heat exchangers [14], solar absorbers [15,16]. Microcellular Si–SiC ceramics can open new fields of applications not yet exploited by their macro cellular counterparts such as thermal partial oxidation (TPOX) reformers and concentrated solar receivers [17].

SiC-based ceramic cellular foams have been produced from few techniques so far [18,19]: direct foaming of a liquid slurry, burn-out of volatile pore formers, and replica. Replica is very effective for producing macro cellular foams with very large pores. However, it becomes ineffective for smaller pores ($<$ 2 mm diameter), since the replication slurry can obstruct cells' windows due to its high viscosity. An alternative route to produce SiC foams is by conversion of carbon foams. This conversion can be carried out by carbo-thermal reduction [20] or by reaction bonding (RB).

The latter technique is attractive since it is the most industrialised manufacturing process of SiC components and their composites [21]. Unlike replica methods, RB takes advantage of the direct foaming technique employed to produce foams having small pores [19]. Different approaches have been used, which differ mainly by the nature of the carbon pristine foam: mesophase pitch foams [22] or resin impregnation of polyurethane foams followed by carbonisation and Si vapour reaction [23].

We present is this work an approach in which microcellular Si–SiC foams were prepared from tannin-based template foam, a new kind of highly porous, cellular solid, natural at the 90% level [24–26]. Condensed (catechic) tannins are commercial bark extracts whose main applications are leatherwork and chemical industry [27]. However, since they are phenolic oligomers, they are also able to react with furfuryl alcohol and formaldehyde. Doing so, high-quality furanic resins are obtained that can be used as such for wood gluing [28] or be foamed in the presence of blowing agent, thus leading to rigid foams [29]. The latter possess high porosity and physical properties that are similar to those of the presently commercialised phenolic foams. Especially, they can have simultaneously very low density and good mechanical properties [24], very low thermal conductivity [30] and outstanding fire resistance [31–33].

Advantages of tannins are manifold: they are abundant, renewable, non-toxic, ecological and inexpensive. After pyrolysis, flawless, vitreous carbon foams with pore sizes within the range of 200 μm are obtained. Conversion into SiC foams was carried out in the present work by putting tannin-derived template foams in contact with silicon or silicon compounds, either in the liquid or in the vapour phase. For that purpose, different experimental approaches have been tested for the first time with such kind of natural precursors.

The paper is organised as follows. Section 2 deals with the preparation of tannin-derived organic and carbon foams, and describes the investigation tools that have been used. Structural and physicochemical characteristics such as porosity, crystallite size, homogeneity, composition, crystalline structure and oxidation resistance derived from SEM, mercury porosimetry and helium pycnometry, XRD, Raman spectroscopy and TGA are considered in section 3. We show that the preparation method has a dramatic impact on both structure and properties of the resultant Si–SiC foams, and that both direct and indirect molten Si infiltration were successful though further optimisation is still required.

2. Experimental

2.1. Foam preparation

In the present work, condensed tannins obtained by spray drying of aqueous Mimosa (*Acacia mearnsii*, De Wild) bark extracts have been used. A liquid mixture made of water (6 g), formaldehyde (7.4 g of 37% water solution), furfuryl alcohol (10.5 g) and diethyl ether (3 g) was first prepared in a 500 mL beaker. The role of each ingredient has been explained elsewhere [25]. The liquid phase was added to tannin powder (30 g), and the whole was strongly stirred. After homogenisation, an acidic catalyst, para-toluene-4-sulphonic acid (11 g of 65% water solution) was added and mixed. A few tens of seconds later, diethyl ether started to boil because of the heat generated by polymerisation of both tannin and furfuryl alcohol, causing a spectacular rising of the foam. Dark, hard, but lightweight blocks having a density of 0.065 g cm^{-3} were obtained and left for age during 24 h.

The outer skin of the material was finally removed, so that only the centre of such big, cylindrical, foams was recovered. The maximum size was corresponding to cubes of side 3 cm, within which samples were subsequently cut off (see subsection 3.1 below). Depending on the methods used for preparing Si–SiC foams (see below), the resultant samples were either used as such, i.e. in the "green" state, or after pyrolysis, i.e. in the form of vitreous carbon. The latter was obtained by simply heating green foams under high purity nitrogen at 4 °C min^{-1} up to 900 °C. The final temperature was maintained during 2 h before cooling under nitrogen flow. Description and properties of carbon foams have been detailed elsewhere [34,35].

Four methods have been tested for preparing Si–SiC composite foams derived from tannin, having their own advantages and drawbacks. For instance, replica with a polymer mitigates the direct RB exothermic reaction [36]:

$$Si_{liquid} + C_{solid} \rightarrow SiC_{solid} \quad \Delta H = = -73 \text{ kJ mol}^{-1}$$

which can deteriorate the strut material. However, due the small pore size of the present foams, the viscous polymer might occlude the pores.

The first method, referred to as method #1, consisted in impregnating green foam samples with preceramic polymer and pyrolysing the resultant material. Two common SiC preceramic liquid polymers with different viscosities were utilised: Starfire SMP 10 (StarPCS SMP-10, Starfire

System, USA) on one hand, which is an allylhydridopolycarbosilane (AHPCS) polymer resin, and KION PSZ20 (Ceraset® Polysilazane 20, Clariant, Switzerland) on the other hand, which is a patented liquid polysilazane. Additional information about these materials is available elsewhere [37,38]. Foam samples were impregnated by one or the other polymer in vacuum for 15 min, then centrifuged at 2500 rpm for 2 min in order to drain the excess polymer. Finally, the samples were pyrolysed at 1000 °C under high-purity argon flowing at 300 $cm^3\ min^{-1}$. The detailed pyrolysis heat ramp is presented in Table 1. Some samples were infiltrated once (1_KION and 1_SF), some others twice (2_KION and 2_SF), with the aforementioned polymers, as shown in Table 2.

The second method (#2 in Table 2) was similar to the previous one using only one single step of polymer impregnation, but an additional step of infiltration with molten silicon was added at the end. For that purpose, the same amount in weight of the foam was placed as Si lumps onto the foam before loading it into the furnace for thermal treatment. Then foams were brought under vacuum (10^{-2} mbar) at temperatures of 1450 °C for 1 h. The aim of doing so was to test the reactivity of the remaining carbon with liquid Si, which might have reacted violently, as suggested above. The SiC already present in the foam was expected to mitigate the exothermic reaction between silicon and carbon.

Method #3 was the direct infiltration of carbon foam with molten silicon, using the same experimental conditions as for method #2. Finally, method #4 was an attempted liquid silicon infiltration (LSI) into vitreous carbon foam through the use of a carbon felt, thus avoiding the direct contact of the carbon foam with liquid Si as described elsewhere [39]. The various samples and the different preparation ways are listed in Table 2.

Table 1
Conditions of pyrolysis for materials prepared by method #1 (impregnation of organic foams with preceramic polymers).

Temperature (°C)	Heating rate (°C h^{-1})	Ramp time (h)	Total elapsed time (h)
21–500	40	11	11
500–1000	60	8	19
1000	Dwell	1	20
1000–21	Power off	~ 24	~ 44

2.2. Characterisation of foams

Foam samples were attached on aluminium sample holders with double-side adhesive carbon tabs (Plano, Wetzlar, Germany) and sputtered with gold. The SEM micrographs were obtained with a Quanta 200 SEM (FEI, Brno, Czech Republic) operated at 20 kV.

Crystalline phase compositions were measured by X-ray diffraction method (XRD). The powder patterns were recorded between 5° and 70° using a Kristalloflex D500 (Siemens, Karlsruhe, Germany), operated with monochromated Cu-Kα radiation (λ = 0.14505 nm, 30 kV, 30 mA).

For one sample only, 2_EN, which was simultaneously available in large amounts, crack-free and flawless, bulk density ρ_b was determined by weighing a big parallelepiped sample of known dimensions ($3 \times 3 \times 1.5\ cm^3$). The skeletal density ρ_s was measured by helium pycnometry (Accupyc II 1340, Micromeritics, USA). For that purpose, sample pieces were crushed in a mortar and dried at 120 °C in vacuum overnight. Each determination included 10 helium flushes prior to analysis, in order to clean the volume chamber of the pycnometer, followed by 50 analytical runs. The overall porosity Φ was calculated as $\Phi = 1 - \rho_b/\rho_s$.

The pore size distribution was estimated by mercury porosimetry (AutoPore IV 9500, Micrometrics, USA). The experiments were performed in two steps: low pressure (0.001–0.24 MPa) and high pressure (0.24–414 MPa). This method was used to get information on pores wider than 3.6 nm, using the well known Washburn equation $D = -4\ \gamma \cos\theta / P$, in which D (nm) is the pore diameter, P (MPa) is the pressure of mercury, and γ (485 mJ m^{-2}) and θ (140°) are surface tension and contact angle of mercury, respectively.

The ceramic foams were also analysed by confocal Raman microscopy (Almega XR, Thermo Fischer, Dreieich, Germany) using a 532 nm laser. The spectra were collected between 250 and 1850 cm^{-1}.

Thermogravimetric analysis (Netzsch 409, Selb, Germany) (TGA) experiments were carried out in dry air for

Table 2
List of samples and detailed conditions of preparation for getting Si–SiC composite foams derived from tannin-based foams.

# Method	Sample ID	Foam precursor		Infiltration agent(s)	Mass after polymer infiltration (g)	Mass after pyrolysis at 1000 °C (g)	Mass after molten Si infiltration (g)
		Kind	Initial mass (g)				
1	1_KION	Green	0.27	KION PSZ20 polymer	1.21	0.86	n.a.
	2_KION	Green	0.23	KION PSZ20 polymer	1.62	0.97	n.a.
1	1_SF	Green	0.24	Starfire SMP 10 polymer	2.3	0.94	n.a.
	2_SF	Green	0.21	Starfire SMP 10 polymer	2.41	0.99	n.a.
2	3_KION	Green	0.14	KION followed by molten Si	1.01	0.56	0.32
	3_SF	Green	0.14	Starfire followed by molten Si	0.84	0.65	0.67
3	1_ER	Carbon	1.14	Molten Si	n.a.	n.a.	1.86
4	2_EN	Carbon	n.a.	Attempted LSI	n.a.	n.a.	n.a.

estimating the resistance to oxidation of the Si–SiC foams. For that purpose, the temperature was increased at 3 °C min^{-1} up to 1400 °C. The absence of moisture was cautiously controlled, because water vapour might lead to the evolution of Si in the form of volatile $Si(OH)_4$. In a typical experiment, 50 mg of foam sample were used.

Finally, thermal conductivity of 2_EN sample was measured at room temperature by the transient plane source method (Hot Disk TPS 2500, ThermoConcept, France). Such sample was chosen because of its big size, making the measurement easy and reproducible. The method is based on a transiently heated plane sensor, used both as a heat source and as a dynamic temperature sensor. It consists of an electrically conducting pattern in the shape of a double spiral, which has been etched out of a thin nickel foil and sandwiched between two thin sheets of Kapton®. The plane sensor was fitted between two identical pieces of foam sample, each one with a flat surface facing the sensor. The dimensions of the sample, compared to that of the sensor, were enough for considering the sample as a semi-infinite medium, $3 \times 3 \times 1.5$ cm^3. The thermal conductivity was then calculated with the Hot Disk 6.1 software.

3. Results and discussion

3.1. Porous structure of raw foams and derived cellular ceramics

The structure of both green and tannin-based carbon foams has been described elsewhere [24,25]. During pyrolysis of green tannin foams, weight loss occurs which is exactly compensated by shrinkage, so that the bulk density remains unchanged [25]. Therefore, only the pore size is reduced by ca. 60% [34]. A typical SEM picture of carbon foam of density 0.065 g cm^{-3} is given in Fig. 1. The linear pore density is around 100 ppi, whereas that of the original green foam was 40 ppi, on average. The tannin—based carbon foam has been successfully modelled as a close packing of spherical pores, having an average coordination number of 12 [40]. It is important to note that the struts are solid and present a triangular cross-section, see Fig. 1(b).

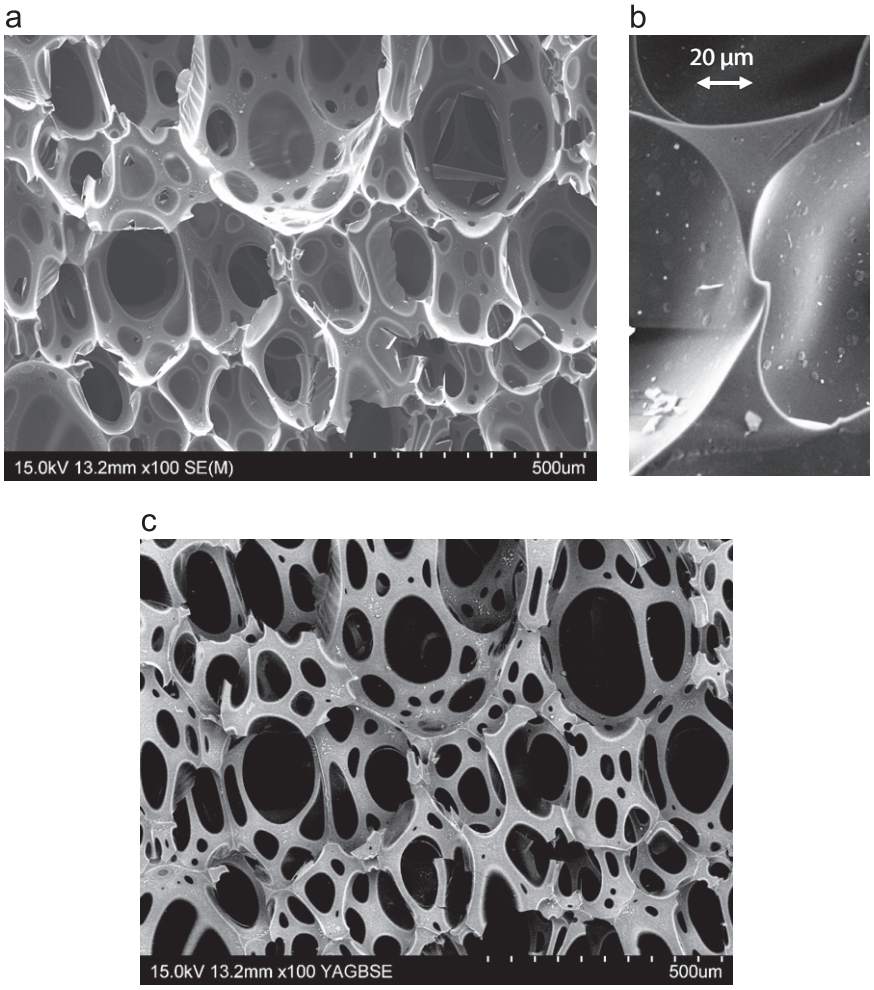

Fig. 1. SEM pictures of carbon foam of density 0.065 g cm^{-3}: (a) Image from secondary electrons best showing pore walls and membranes between cells; (b) Cross-section of two struts; (c) Same as (a), but from backscattered electrons best showing pore windows and struts.

Given the skeletal density of tannin-based resin and vitreous carbon, 1.59 and 1.98 g cm^{-3}, respectively [25], green and carbon foam samples present total porosities of 96–97%. These values suggest that a high volume fraction of tannin foams may be impregnated, provided that the connectivity between the cells is good enough. According to Fig. 1 and many other pictures of tannin-based foams, the cells are connected with each other through circular windows. However, some of them are closed by thin membranes. In carbon foams, most membranes are burst, whereas more cells remain closed in green foams. Carbon foams might thus be easier to impregnate, despite their corresponding lower window diameters ranging from 10 to 200 μm.

Taking these arguments into account, the possibility of deeply infiltrating green foams and covering their struts with a viscous preceramic polymer was checked only with small cubic samples having a side close to 1.5 cm. Foams impregnated with polymers indeed presented filled cells at their surface, whereas only partly filled cells were observed in the inner parts. In contrast, infiltration with molten Si was found to be successful and very homogeneous with carbon foam samples having volumes up to 17 cm^3. Selected SEM pictures of Si–SiC foam samples prepared according to the methods investigated here are presented in Fig. 2.

Samples derived from KION were systematically cracked, whereas those made from Starfire polymer were not. These

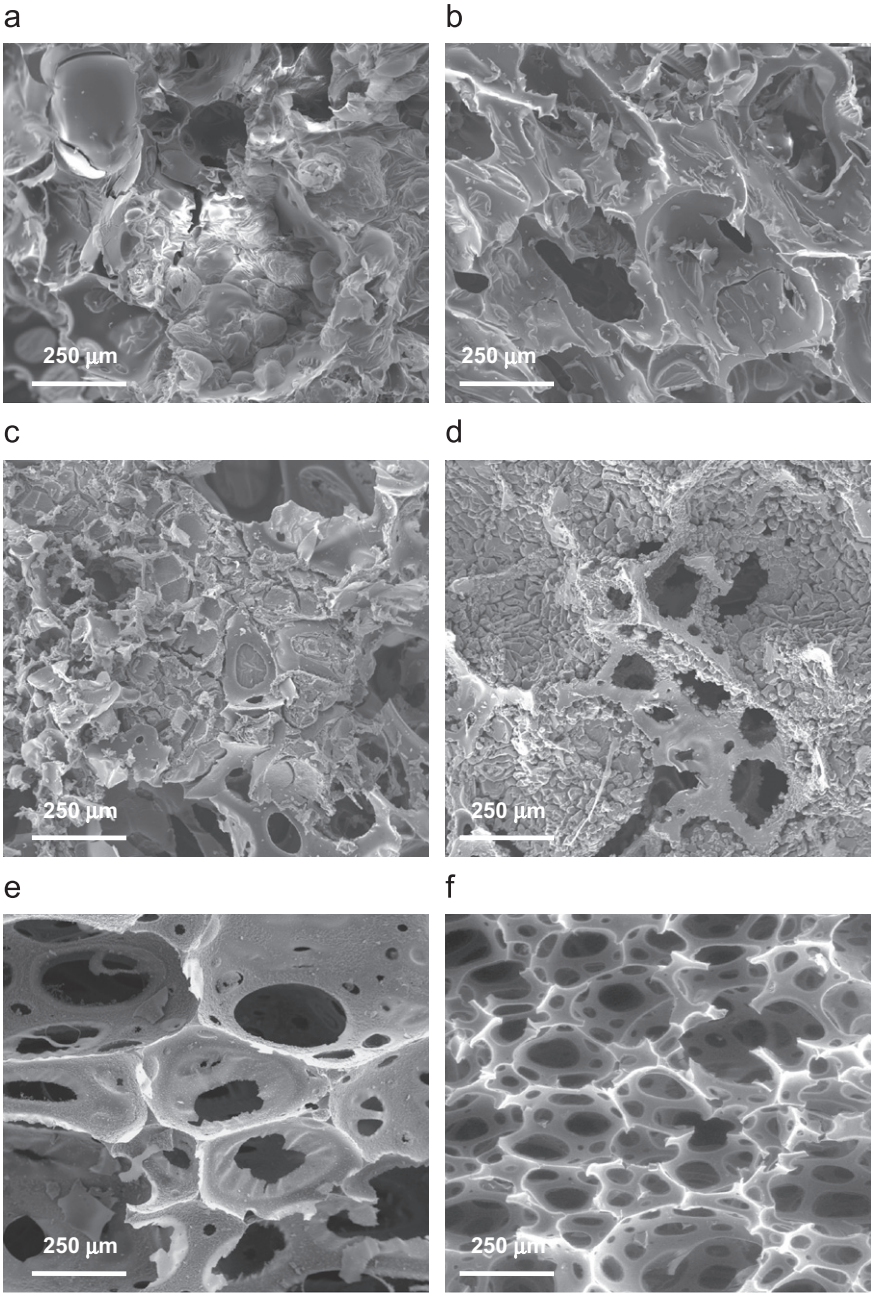

Fig. 2. SEM pictures of Si–SiC composite foams prepared according to different methods (see Table 2): (a) 1_KION; (b) 1_SF; (c) 3_KION; (d) 3_SF; (e) 1_ER; (f) 2_EN.

differences might be due to differential shrinkage between foam and polymer, whose ceramic yield was around 60–70%. It has to be also considered that samples shrinkage continued inside the high-temperature furnace up to the melting point of Si. At these temperatures, both polymers experienced a microstructure re-arrangement and a certain mass loss, especially for KION. This fact explains why, in Table 2, KION samples were lighter after LSI. Different viscosities of the polymers combined to the temperature of cross-linking of Starfire (250–400 °C), which is higher than that of KION (180–200 °C) [37,38], might have an influence. Thus, materials prepared with Starfire looked homogeneous compared to those made from KION (see Fig. 2(a) and (b)), even though filled pores could be observed, with a possible impregnation gradient. All materials prepared with method #1 presented considerable weight uptakes, the initial mass of the foam being multiplied by a factor ranging from 3.2 to 4.7 after conversion into ceramic. The porosity of the corresponding samples has thus been considerably filled and partly blocked by such amount of Si-based material. The same conclusion applies to samples prepared by method #2, see Fig. 2(c) and (d).

Samples infiltrated, directly or not, with molten silicon, presented much more preserved interconnected pore structure, as seen in Fig. 2(e) and (f). This fact may be explained by the correspondingly lower weight increase. The mass of the final ceramic was only 1.6 times higher than that of the initial carbon foam (see Table 2). Such value is two times lower than what is expected for a complete conversion of carbon ($12\ g\ mol^{-1}$) into silicon carbide ($40\ g\ mol^{-1}$). Reaction of Si with carbon thus might not be complete, suggesting that synthesis parameters have to be optimised. Analysis of microstructure will confirm this point.

3.2. Microstructure of Si–SiC composite foams

The surface of each material has been examined in order to determine the SiC grains and therefore estimate the completeness of the siliconization. Surfaces of 1_KION and 1_SF (not shown) were rather smooth locally, whereas those of 2_KION and 2_SF presented heterogeneous dispersion of small grains, as seen in Fig. 3(a). Adding a supplementary step of molten Si infiltration led to very coarse grains, as seen in Fig. 3(b)–(d). Comparing Fig. 3(b) and (c) shows that the grains in 3_SF, around 10 μm in size, were much bigger than those of 3_KION.

Direct infiltration of molten Si led to SiC grains a few μm big (Fig. 3(e)), whereas no grains could be evidenced after indirect infiltration throughout carbon felt (Fig. 3(f)). As already suggested by the moderate weight gained by carbon samples submitted to molten silicon, it appears that the reaction between C and Si was not complete, probably due to a too limited contact time. Due to restricted capillary forces as a consequence of the large pore size, which prevent infiltration of the foams, it is assumed that only very fine grained SiC was formed at the surface of tannin-derived carbon foams. The SiC was most probably produced from the reaction of the substrate with Si vapours, which infiltrate the porous foam as described earlier [41].

XRD patterns of all samples are presented in Fig. 4. All materials made from method #1 appeared to be fully amorphous and no crystalline Si or SiC phase could be detected. The other methods, i.e. #2 to #4, involving a step of molten Si infiltration, all led to crystallised SiC. This finding suggests the relevance of such step for converting tannin-based foam into ceramic. The silicon carbide was crystallised mainly as the cubic 3C-SiC phase (β-SiC), with some hexagonal 6H–SiC phase (α-SiC), which is consistent with earlier observation on biotemplated Si–SiC [41]. Crystalline silicon was also observed in 3_SF and 1_ER, see Fig. 4(b) and (c). Finding an excess of silicon implies that most carbon has been converted into SiC, unlike what happened in the other materials.

Raman spectra shown in Fig. 5 confirmed the previous conclusions: foams derived from preceramic polymer impregnation (method #1) were all totally amorphous, and neither SiC nor Si could be detected. In contrast, both Si and SiC were clearly evidenced in foams prepared with method #2. 3_KION indeed presented no carbon and a substantial amount of Si, whereas 3_SF presented much less Si and a few residual C. It may thus be concluded that the reaction was more complete for KION impregnation followed by liquid Si infiltration (Fig. 5(a) and (b)). When only molten Si was used for converting carbon foams into SiC, the presence of the latter was systematically confirmed by Raman. Direct infiltration (1_ER) led to nicely crystallised SiC with some residual Si and C (Fig. 5(c)). As explained above, tannin-based carbon foams have solid struts, so their conversion into SiC was expected to be uneasy. Moreover, vitreous carbon is not so well wetted by liquid Si, compared to graphite, the contact angle being 50° at 1450 °C [42]. Finding simultaneously Si and C suggests that some thick parts of the struts were converted only superficially into SiC. In the case of 2_EN (indirect infiltration), the characteristic D and G bands of carbon were clearly seen, whereas only little 3C–SiC was found. This indicates that the attempted LSI did not occur. However, according to previous results [41], Si vapours are able to pass through the porous foam template, leading to a surface conversion of the carbon into the observed SiC [43]. These findings might also explain the results obtained from the SEM investigations. Consequently, most of the carbon of the tannin-derived foam is still unreacted, whereas thin layer of SiC was formed at the surface of the struts.

3.3. Oxidation resistance of Si–SiC composite foams

Thermogravimetry curves of samples heated in dry air at $3\ °C\ min^{-1}$ up to 1400 °C are presented in Fig. 6. Composite foams were remarkably stable, even at high temperature. SiC is indeed expected to oxidise above 1200 °C, whereas Si oxidises at much lower temperature. Weight losses were evidenced for all materials at temperatures increasing up to around 800 °C, indicating that all contained residual carbon that has been burnt in air. Fig. 6(a)

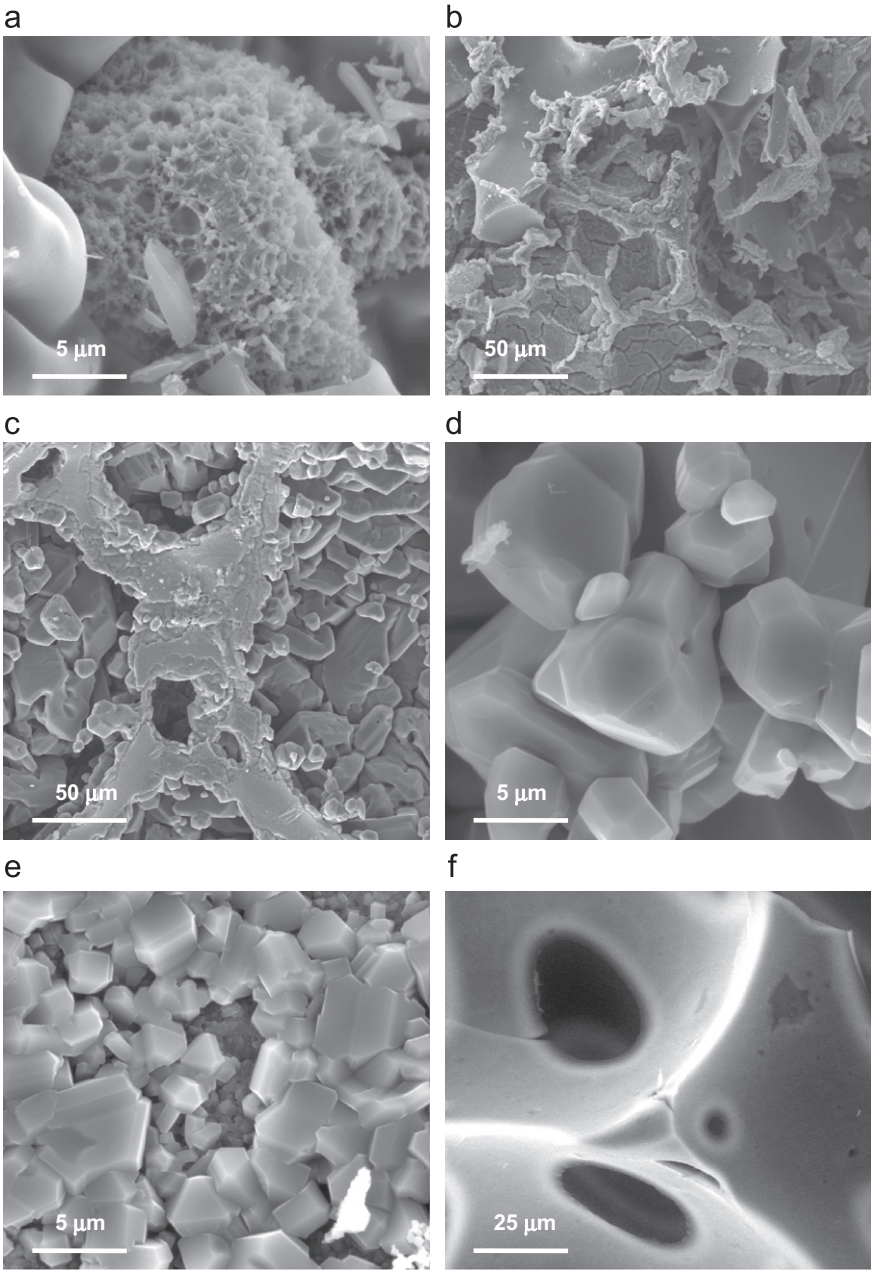

Fig. 3. Same as Fig. 2, but at higher magnification for estimating the size of SiC grains: (a) 2_SF; (b) 3_KION; (c) and (d) 3_SF; (e) 1_ER; (f) 2_EN.

clearly shows that the amount of residual carbon in 1_KION was higher than in 2_KION and 3_KION, but similar to that of 1_SF and 2_SF. 3_SF (see Fig. 6(b)) was the sample which lost the lowest weight, only 3%, suggesting that only a few carbon was remaining and that a significant amount of Si has been left by infiltration. Accordingly, a fast weight increase was observed above 1000 °C, indicating the oxidation of the excess Si, followed by that of SiC. The same conclusion also applies to 3_KION.

In agreement with the previous findings from XRD and Raman, C, Si and SiC were all present in 1_ER (see Fig. 6(c)). However, the amount of carbon remaining in the structure was unexpectedly high, given that around 45% of the initial mass has been lost below 800 °C. Despite the significant amount of SiC observed in Fig. 3(e), the correspondingly coarse grains did not protect the residual carbon against oxidation. The same was found for 2_EN, whose amount of very thin-grained SiC was definitely too low for offering a good protection from oxidation at high temperature.

3.4. Focus on 2-EN sample: porosity and thermal conductivity

As explained in the experimental section, only small samples have been prepared except for 2_EN, for which additional measurements could be done. The bulk density

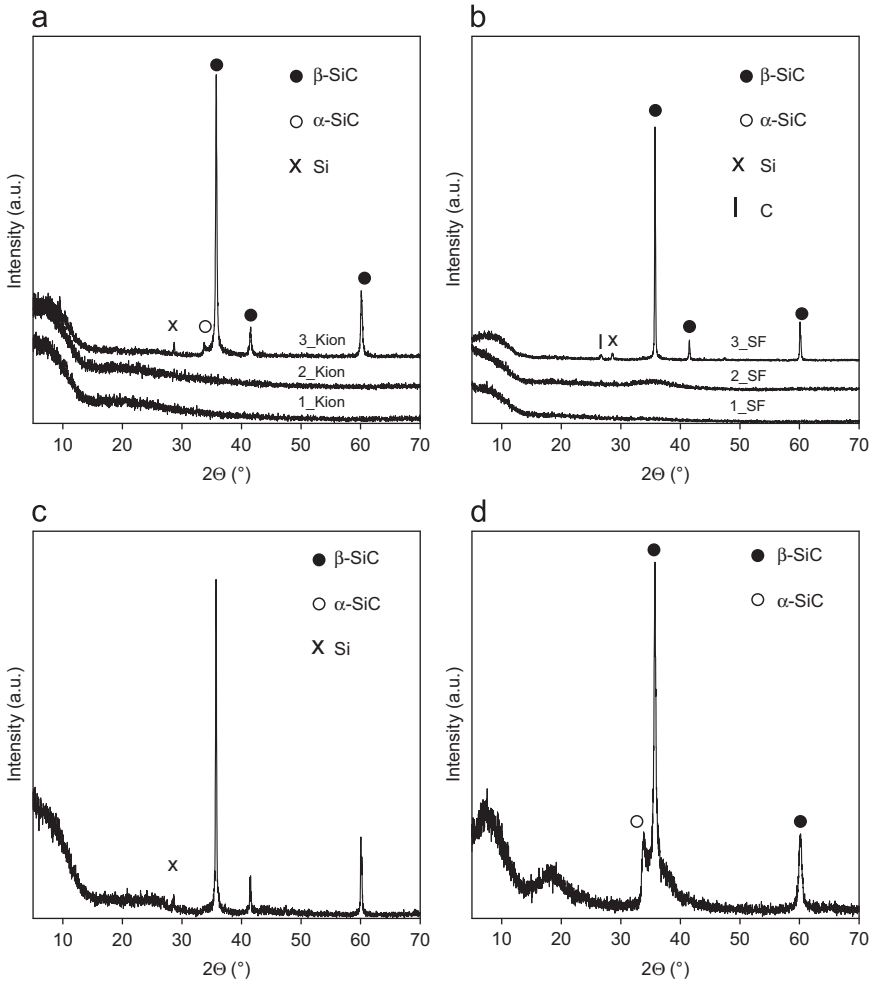

Fig. 4. XRD patterns of all composite Si–SiC foams investigated here: (a) Samples derived from KION polymer; (b) Samples derived from Starfire polymer; (c) 1_ER; (d) 2_EN.

was 0.086 g cm^{-3}, whereas helium pycnometry led to a value of 2.13 g cm^{-3} for the skeletal density. The latter value is much lower than the expected density of pure SiC, 3.21 g cm^{-3}. Such result further confirms the incomplete conversion of C into SiC during the LSI trial. From the measured density values, the overall porosity could be deduced: 96.0%. Mercury porosimetry led to additional information such as pore size distribution, which is presented in Fig. 7. The maximum of the distribution at 190 μm is close to the average cell diameter observed by SEM in the original carbon foams (see Fig. 1(c)), as well as in Si–SiC foam (see Fig. 2(f)). The other peaks of the distributions correspond to narrower windows which can also be observed in the same pictures.

The thermal conductivity measured at room temperature was 0.67 ± 0.01 W m^{-1} K^{-1}. This value is rather low compared to others taken from the literature, generally much higher than 1 W m^{-1} K^{-1}, even for highly porous foams [44 and refs. therein]. In fact, no equation among the long list provided in the review of Collishaw and Evans [45] is able to lead to such low value, taking into account the thermal conductivity of air and cubic 3C–SiC phase (β-SiC) at room temperature: 0.026 and 360 W m^{-1} K^{-1}, respectively. All the calculated results were indeed always much higher than the experimental value. This finding once more supports that the conversion of carbon into SiC has been only superficial, so that 2_EN foam can be seen as a backbone of vitreous carbon coated with SiC. In fact, considering the thermal conductivity of bulk glassy carbon, 3.5 W m^{-1} K^{-1} [46], thermal conductivities ranging from 0.034 to 0.072 W m^{-1} K^{-1} may be calculated for a foam containing 96% of air. Such values are obtained from various equations in which the radiative part was neglected: that of Shuetz and Glicksman [47], considered as one of the best equations describing the thermal conductivity of foams [45], that of Ashby [48], or that of Ahern et al. [49] in which the fraction of solid contained in cell edges was set at 95%, according to previous results from the present authors [50]. A thermal conductivity close to 0.065 W m^{-1} K^{-1} was indeed recently measured at room temperature for tannin–based carbon foams having the same porosity [51]. Finding here a value close to

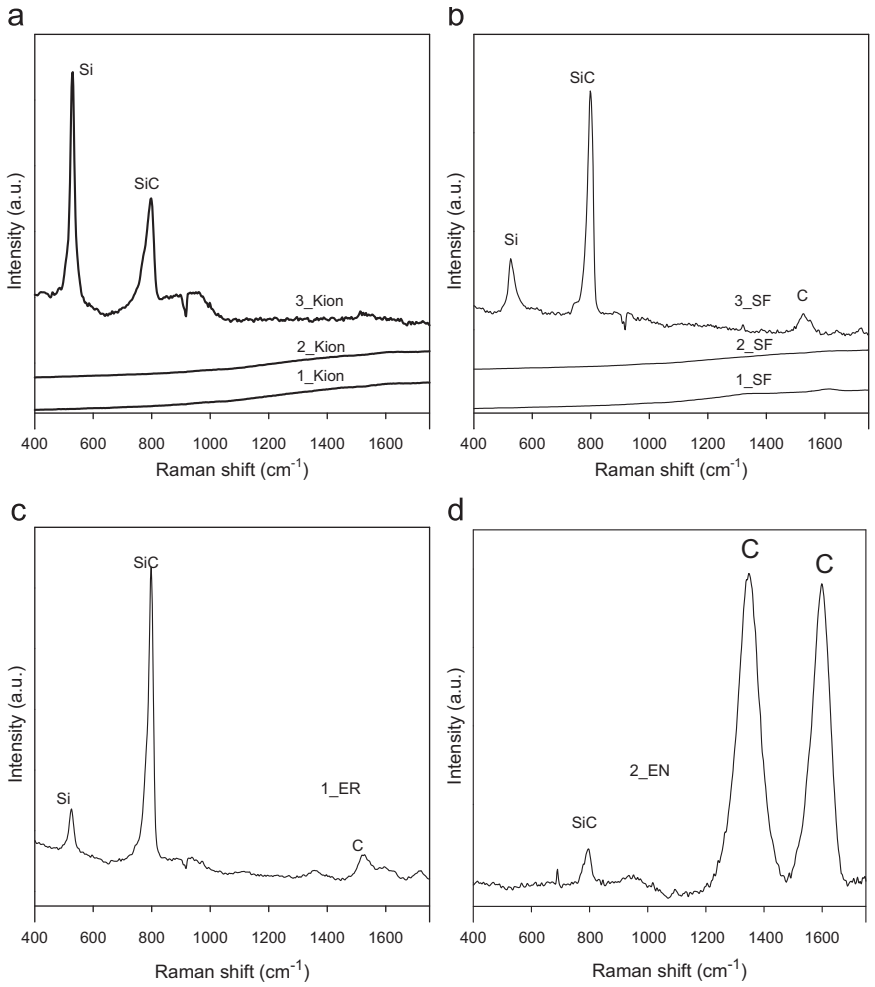

Fig. 5. Raman spectra of all composite Si–SiC foams investigated here.

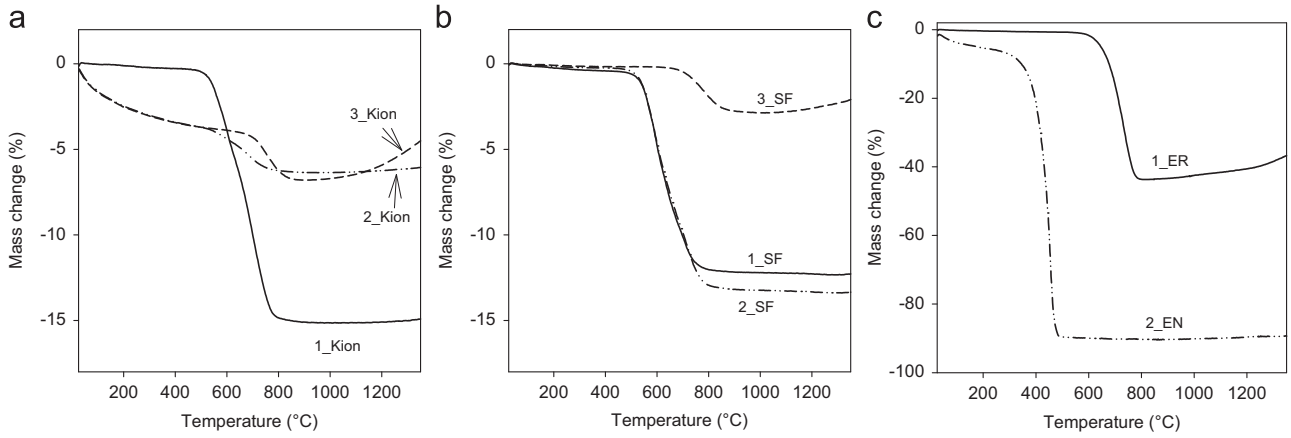

Fig. 6. Thermogravimetry curves of Si–SiC composite foams: (a) Samples derived from KION polymer; (b) Samples derived from Starfire polymer; (c) Samples 1_ER and 2_EN.

$0.7\ W\ m^{-1}\ K^{-1}$ for the sample 2_EN, i.e. 10 times higher than that of pure carbon foam, suggests that the high thermal conductivity of SiC, despite its probably low thickness, could seriously improve the heat transfer within the foam.

4. Conclusion

This work explored for the first time the possibility of preparing Si–SiC microcellular ceramics from foams

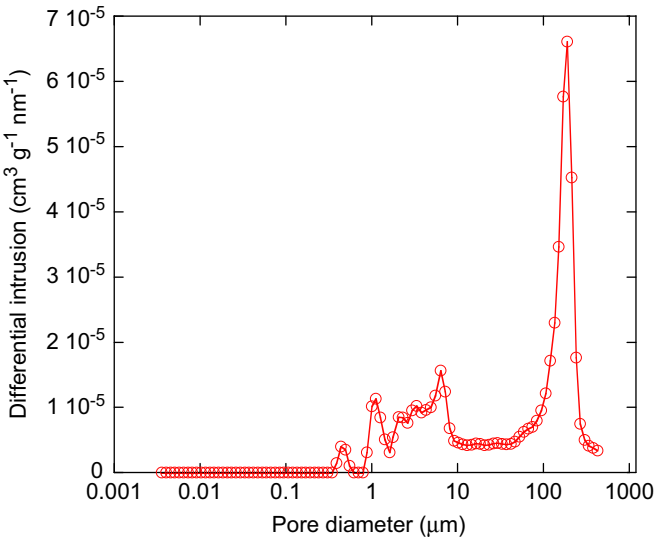

Fig. 7. Pore-size distribution of sample 2_EN as deduced from mercury porosimetry.

templates, organic or carbonaceous, derived from tannins. These precursors present the advantages of being renewable, non-toxic and very cheap, and the corresponding foams have solid struts, unlike what is found in some commercial SiC foams. However, such characteristic also made the sample uneasy to prepare.

Aiming at producing a reticulated SiC foam with a pore size smaller than 200 μm, several experimental techniques were adopted. Replica with low viscosity polymers and pyrolysis led to non reticulated porous structures with low amount of crystalline SiC. However, even if some carbon remained and was able to oxidise, the oxidation protection of the material was good. When additional molten Si infiltration was used, the protection was even better but a significant amount of excess Si was observed in a very heterogeneous porous structure.

Direct liquid infiltration led to reticulated foam with the same structure of the template carbon foam, based on nicely crystallised SiC with some free Si. Its oxidation resistance was worse than the previous foams. Vapour infiltration of Si throughout carbon felt was also successful, and led to a very homogeneous material made of surface thin-grained SiC covering the inner glassy carbon. However, the low amount of SiC grains thus produced did not allow a sufficient protection of the residual carbon against oxidation. Therefore, significant optimisation of all the materials presented in this paper is required. Such studies are presently carried out and should be published in the near future.

Acknowledgements

The authors gratefully acknowledge the financial support of the CPER 2007-2013 "Structuration du Pôle de Compétitivité Fibres Grand'Est" (Competitiveness Fibre Cluster), through local (Conseil Général des Vosges), regional (Région Lorraine), national (DRRT and FNADT) and European (FEDER) funds. The authors gratefully also acknowledge Dr. Tobias Fey, FAU Erlangen—Glass and Ceramics for his technical assistance and many helpful discussions, and the company Erbicol for having performed the siliconization process in their labs.

References

[1] L.J. Gibson, M.F. Ashby, Cellular solids structure and properties, Cambridge University Press, Cambridge, 1999.
[2] T.J. Fitzgerald, V.J. Michaud, A. Mortensen, Processing of microcellular SiC foams. Part II. Ceramic foam production, Journal of Materials Science 30 (1995) 1037–1045.
[3] R.A. Mach, F.v. Issendorff, A. Delgado, A. Ortona, Experimental investigation of the oxidation behavior of Si–SiC-foams, in: R. Narayan, P. Colombo (Eds.), Advances in Bioceramics and Porous Ceramics, Vol. 29, John Wiley & Sons Inc., Hoboken, 2009, pp. 299–311.
[4] A. Ortona, S. Pusterla, P. Fino, F.R.A. Mach, A. Delgado, S. Biamino, Ageing of reticulate Si–SiC foams in porous burners, Advances in Applied Ceramics 109 (2010) 246–251.
[5] M. Ashby, Hybrid materials to expand the boundaries of material-property space, Journal of the American Ceramic Society 94 (2011) S3–S14.
[6] A. Ortona, S. Gianella, D. Gaia, SiC foams for high temperature applications, in: R. Narayan, P. Colombo, S. Widjaja, D. Singh (Eds.), Advances in Bioceramics and Porous Ceramics IV: Ceramic Engineering and Science Proceedings, Vol. 32, John Wiley & Sons Inc., Hoboken, NJ, 2011, pp. 153–162.
[7] M. Scheffler, P. Colombo, Cellular ceramics: structure, manufacturing, properties and applications, Wiley-VCH Verlag GmbH, Weinheim, 2005.
[8] D. Trimis, F. Durst, Combustion in porous medium—advances and applications, Combustion Science and Technology 121 (1996) 153–168.
[9] D. Trimis, Porenbrennertechnologie—Ein Überblick [Porous burner technology—An overview], GWF, Gas—Erdgas 147 (2006) 92–99.
[10] S. Wood, A.T. Harris, Porous burners for lean-burn applications, Progress in Energy and Combustion 34 (2008) 667–684.
[11] M. Abdul Mujeebu, M.Z. Abdullah, M.Z. Abu Bakar, A.A. Mohamad, M.K. Abdullah, Applications of porous media combustion technology—a review, Applied Energy 86 (2009) 1365–1375.
[12] M.V. Twigg, J.T. Richardson, Fundamentals and applications of structured ceramic foam catalysts, Industrial and Engineering Chemistry Research 46 (2007) 4166–4177.
[13] J. Grosse, B. Dietrich, G. Incera Garrido, P. Habisreuther, N. Zarzalis, H. Martin, M. Kind, B. Kraushaar-Czarnetzki, Morphological characterization of ceramic sponges for applications in chemical engineering, Industrial and Engineering Chemistry Research 48 (2009) 10395–10401.
[14] A. Ortona, S. Pusterla, S. Gianella, An integrated assembly method of sandwich structured ceramic matrix Composites, Journal of the European Ceramic Society 31 (2011) 1821–1826.
[15] T. Fend, High porosity materials as volumetric receivers for solar energetic, Optica Applicata 40 (2010) 271–284.
[16] M. Roeb, D. Thomey, D. Graf, L. de Oliveira, C. Sattler, S. Poitou, F. Pra, P. Tochon, A. Brevet, G. Roux, N. Gruet, C. Mansilla, F. LeNaour, R. Allen, R. Elder, I. Atkin, G. Kargiannakis, C. Agra_otis, A. Zygogianni, C. Pagkoura, A.G. Konstandopoulos, A. Giaconia, S. Sau, P. Tarquini, T. Kosmidou, P. Hähner, S. Haussener, A. Steinfeld, I. Canadas, A. Orden, M. Ferrato, HycycleS—A Project on Solar and Nuclear Hydrogen Production by Sulphur-based Thermochemical Cycles, in: D. Stolten, T. Grube (Eds.), World Hydrogen Energy Conference 2010—WHEC2010 Proceedings, Essen, 2010, pp. 267–274.

[17] S. Gianella, D. Gaia, A. Ortona, High Temperature Applications of Si–SiC Cellular Ceramics, Advanced Engineering Materials, WILEYVCH Verlag, 2012 published online.
[18] P. Colombo, Conventional and novel processing methods for cellular ceramics, Philosophical Transactions of the Royal Society A 364 (2006) 109–124.
[19] A.R. Studart, U.T. Gonzenbach, E. Tervoort, L.J. Gauckler, Processing routes to macroporous ceramics: a review, Journal of the American Ceramic Society 89 (2006) 1771–1789.
[20] Y.W. Kim, C.B. Park, Processing of microcellular preceramics using carbon dioxide, Composites Science and Technology 63 (2003) 2371–2377.
[21] A. Ortona, Ceramic Matrix Composites: Reaction Bonded, in: Wiley Encyclopedia of Composites, John Wiley & Sons Inc, 2011.
[22] Z. Zhang, F. Wang, X. Yu, Y. Wang, Y. Yan, Porous silicon carbide ceramics produced by a carbon foam derived from mixtures of mesophase pitch and Si particles, Journal of the American Ceramic Society 92 (2009) 260–263.
[23] Y. Aoki, B. McEnaney, SiC foams produced by siliciding carbon foams, British Ceramic Transactions 94 (1995) 133–137.
[24] G. Tondi, W. Zhao, A. Pizzi, G. Du, V. Fierro, A. Celzard, Tannin-based rigid foams: a survey of chemical and physical properties, Bioresource Technology 100 (2009) 5162–5169.
[25] W. Zhao, V. Fierro, A. Pizzi, G. Du, A. Celzard, Effect of composition and processing parameters on the characteristics of tannin-based rigid foams. Part I: cell structure, Materials Chemistry and Physics 122 (2010) 175–182.
[26] W. Zhao, A. Pizzi, V. Fierro, G. Du, A. Celzard, Effect of composition and processing parameters on the characteristics of tannin-based rigid foams. Part II: physical properties, Materials Chemistry and Physics 123 (2010) 210–217.
[27] A. Pizzi, Tannins: Major Sources, Properties and Applications, in: M.N. Belgacem, A. Gandini (Eds.), Monomers, Polymers and Composites from renewable Resources, Oxford, 2008, pp. 179–199.
[28] A. Pizzi, Advanced Wood Adhesives Technology. M. Dekker Inc, New York, 1994.
[29] N.E. Meikleham, A. Pizzi, Acid- and alkali-catalyzed tannin-based rigid foams, Journal of Applied Polymer Science 53 (1994) 1547–1556.
[30] M.C. Basso, X. Li, V. Fierro, A. Pizzi, S. Giovando, A. Celzard, Green, formaldehyde-free, foams for thermal insulation, Advanced Materials Letters 2 (2011) 378–382.
[31] A. Celzard, V. Fierro, G. Amaral-Labat, A. Pizzi, J. Torero, Flammability assessment of tannin-based cellular materials, Polymer Degradation and Stability 96 (2011) 477–482.
[32] G. Tondi, A. Pizzi, H. Pasch, A. Celzard, K. Rode, MALDI-ToF investigation of furanic polymer foams before and after carbonization: aromatic rearrangement and surviving furanic structures, European Polymer Journal 44 (2008) 2938–2943.
[33] G. Tondi, A. Pizzi, H. Pasch, A. Celzard, Structure degradation, conservation and rearrangement in the carbonisation of polyflavonoid tannin/furanic rigid foams: a MALDI-TOF investigation, Polymer Degradation and Stability 93 (2008) 968–975.
[34] G. Tondi, V. Fierro, A. Pizzi, A. Celzard, Tannin based Carbon Foam, Carbon 47 (2009) 1480–1492.
[35] G. Tondi, V. Fierro, A. Pizzi, A. Celzard. Erratum to Tannin-based carbon foam [Carbon 47 (2009) 1480–1492], Carbon 47 (2009) 2761.
[36] M.W. Chase Jr, NIST-JANAF Thermochemical Tables, J. Phys. Chem. Ref. Data 9 (1998) 1–1951 Monograph.
[37] Starfire SMP-10 Datasheet, 〈http://www.starfiresystems.com/docs/ceramic-forming-polymers/SMP-10.pdf 〉, (accessed 06.07.12).
[38] Ceraset® Polysilazane 20 Datasheet, Clariant, 〈http://www.kioncorp.-com/datasheets/Ceraset%20Polysilazane%2020%20Product%20Bulletin.pdf〉, (accessed 06.07.12).
[39] C. Zollfrank, H. Sieber, Microstructure and phase morphology of wood derived biomorphous SiSiC-ceramics,, European Ceramic Society 24 (2004) 495–506.
[40] G. Tondi, S. Blacher, A. Léonard, A. Pizzi, V. Fierro, J.M. Leban, A. Celzard, X-ray microtomography studies of tannin-derived organic and carbon foams, Microscopy and microanalysis : The Official Journal of Microscopy Society of America, Microbeam Analysis Society, Microscopical Society of Canada 15 (2009) 384–394.
[41] C. Zollfrank, H. Sieber, Microstructure evolution and reaction mechanism of biomorphous SiSiC-ceramics, Journal of the American Ceramic Society 88 (2005) 51–58.
[42] T.J. Whalen, A.T. Anderson, Wetting of SiC, Si_3N_4, and carbon by Si and binary Si alloys, Journal of the American Ceramic Society 58 (1975) 396–399.
[43] E. Vogli, H. Sieber, P. Greil, Biomorphic SiC-ceramic prepared by Si-vapour phase infiltration of wood, Journal of the European Ceramic Society 22 (2002) 2663–2668.
[44] A. Ortona, S. Pusterla, S. Valton, Reticulated SiC foam X-ray CT, meshing and simulation, in: 34th International Conf and Exposition on Advanced Ceramics and Composites Procedings (ICACC 2010), Daytona Beach, FL, USA, 2010.
[45] P.G. Collishaw, J.R.G. Evans, An assessment of expressions for the apparent thermal conductivity of cellular materials, Journal of Materials Science 29 (1994) 2261–2273.
[46] M. Bastick, P. Chiche, J. Rappeneau, La texture des carbones, in: Eds., in: Carbones Les (Ed.), Groupe Français d'Etude des Carbones, 2, Masson et Cie, Paris, 1965, p. 208.
[47] M.A. Shuetz, L.R. Glicksman, A basic study of heat transfer through foam insulation, Journal of Cellular Plastics 20 (1984) 114–121.
[48] M.F. Ashby, The properties of foams and lattices, Philosophical Transactions of the Royal Society A 364 (2006) 15–30.
[49] A. Ahern, G. Verbist, D. Weaire, R. Phelan, H. Fleurent, The conductivity of foams: a generalisation of the electrical to the thermal case, Colloids and Surfaces A-Physicochemical and Engineering Aspects 263 (2005) 275–279.
[50] A. Celzard, W. Zhao, A. Pizzi, V. Fierro, Mechanical properties of tannin—based rigid foams undergoing compression, Materials Science and Engineering A 527 (2010) 4438–4446.
[51] X. Li, M.C. Basso, F.L. Braghiroli, V. Fierro, A. Pizzi, A. Celzard, Tailoring the structure of cellular vitreous carbon foams, Carbon 50 (2012) 2026–2036.